Daily and hourly chemical impact of springtime transboundary aerosols on Japanese air quality

good title

T. Moreno[1], T. Kojima[2], F. Amato[3], F. Lucarelli[4], J. de la Rosa[5], G. Calzolai[4], S. Nava[4], M. Chiari[4], A. Alastuey[1], X. Querol[1] and W. Gibbons[6]

[1]{Inst. of Environmental Assessment & Water Research (IDÆA-CSIC), Jordi Girona 18, 08034 Barcelona, Spain}

[2]{Dept. of Earth & Environmental Sciences, Kumamoto University, Kurokami, Kumamoto 860-8555, Japan}

[3]{TNO Climate, Air and Sustainability, Princetonlaan 6, PO Box 80015, 3508 TA Utrecht, The Netherlands}

[4]{Dept. of Physics and Astronomy, University of Florence, and INFN, Sesto Fiorentino, Florence I-50019, Italy}

[5]{Center for Research in Sustainable Chemistry (CIQSO), University of Huelva, Campus de El Carmen, s/n, 21071 Huelva, Spain}

[6]{AP 23075, Barcelona 08080, Spain}

Abstract

The regular eastward drift of transboundary aerosol intrusions from the Asian mainland into the NW Pacific region has a pervasive impact on air quality in Japan, especially during springtime. Analysis of 24-hour filter samples (ICP-AES and ICP-MS) and hourly Streaker (PIXE) samples reveal the chemistry of successive waves of natural mineral desert dust ("*Kosa*") and metalliferous sulphatic pollutants arriving in western Japan during spring 2011. The main aerosol sources recognised by PMF analysis of Streaker data are mineral dust and fresh sea salt (both mostly in the coarser fraction $PM_{2.5-10}$), As-bearing sulphatic aerosol ($PM_{0.1-2.5}$), metalliferous sodic PM interpreted as aged, industrially contaminated marine aerosol, and ZnCu-bearing traffic-related emissions. Whereas mineral dust arrivals are typically highly transient, peaking over a few hours, sulphatic intrusions build up and decline more slowly, and are accompanied by notable rises in ambient concentrations of metallic trace elements such as Pb, As, Zn, Sn and Cd. The magnitude of the loss in regional air quality due to the spread and persistence of pollution from mainland Asia is especially clear when cleansing oceanic air advects westward across Japan, removing the continental influence and reducing concentrations of the ~~more~~ undesirable metalliferous pollutants by over 90%.

possibly local

?

are they really cleansing, or simply dilute or displace the polluted air mass.

All the acronyms should be given in full first time used. ICP-AES, ICP-MS and PIXE are well known; PMF and PM more obscure.

Keywords: Transboundary atmospheric pollution; Japan air quality; Arsenic, sulphatic aerosols.

1 Introduction

The spectacular growth of the Chinese economy in recent years has been accompanied by an equally impressive deterioration in regional air quality (Liu and Mauzerall, 2007; Ohara et al., 2007; Chan and Yao, 2008; Aikawa et al., 2010). The problem is on such a scale that a plume of particulate matter (PM) rich in secondary inorganic compounds (SIC) regularly contaminates millions of square kilometres across the NW Pacific region and beyond (Prospero et al., 2003; Liu et al., 2008; Fairlie et al., 2010; Moreno et al., 2012). The Japanese archipelago and the Korean Peninsula are especially affected by these transboundary aerosol intrusions. A common scenario is for stagnant anticyclonic conditions over central China concentrating pollutants which later become transported oceanward, sometimes mixing with Gobi desert dust blown in from the NW (Guo et al., 2004; Ma et al., 2004; Uno et al., 2004; Wang et al., 2004; Chung and Kim, 2008; Zhang et al., 2010; Takahashi et al., 2010). The exportation of the resulting aerosol cocktail (Fig. 1) is so frequent as to create in Japan what has been described as a "quasi-permanent" state of regional atmospheric pollution (Lasserre et al., 2008) and has led inevitably to concerns over possible health effects on the Japanese population (e.g. Ichinose et al., 2005; Ueda et al., 2010; Watanabe et al., 2010; Onishi et al., 2012). However there is still a relative paucity of detailed information published on the variations in chemical concentrations of the aerosols people are inhaling during these transboundary pollution events.

With the above observation in mind in 2010 we conducted a pilot campaign to analyse 24-hour PM_{10} filters collected during three transient transboundary pollution episodes crossing western Japan. Our results confirmed the pronounced bimodality and inhomogeneity between natural and anthropogenic PM in East Asian transboundary aerosol intrusions (Moreno et al., 2012). Furthermore, although the number of filters analysed was relatively small, it was nevertheless enough to demonstrate the highly metalliferous and chemically complex nature of sulphatic plumes arriving from industrial China. Such plumes drift across Japan, creating regional pollution clouds that dissipate only slowly due to the dominance of atmospherically persistent submicron accumulation

The MS would be better with a more detailed map of the collection site, showing coast, industry and nearby major roads.

mode PM. It was this aspect of the chemical data, rather than the already well-characterised nature of the "natural" Gobi-desert derived *Kosa* intrusions, which seemed to us in more urgent need of further study. In this context this ~~present~~ manuscript moves forward by presenting a new database collected during a 6-week period of continuous hourly and daily measurements in Kumamoto, SW Japan. The study adopts an unusually multi-analytical approach by integrating results from Particle Induced X-ray Emission (PIXE), Inductively Coupled Plasma Mass Spectrometry/Atomic Emission (ICPMS/AE) spectroscopy, chromatography and thermal-optical transmission methods, allowing comparison between hourly (Streaker) and 24-hour (filter) data. Such data are unprecedented in the chemical detail they offer on Japanese air chemistry during transboundary aerosol inflows.

this really shows the regional situation

2 Methodology

Samples

~~Data~~ were obtained in March and April 2011 at the top of a nine-storey building within the Kumamoto University precinct on the island of Kyushu in Western Japan (Fig. 1) approximately midway between Tokyo (c. 1000km ENE) and Shanghai (c. 1000km WSW). Kumamoto city is not impacted by any nearby heavy industrial point sources, making it an excellent location to observe the arrival of transboundary aerosol intrusions. The monitoring site can be classified as an urban background site influenced to some extent by road traffic emissions from a city centre arterial road 1400 m to the west and a minor two-lane road crossing the University area.

see comment above

We measured hourly element concentrations continuously from 17th March to 28th April using a Streaker sampler collecting hourly aerosol samples in two size ranges (0.1-2.5 μm and 2.5-10 μm) at an air flow rate of 1 $lmin^{-1}$ that were then analyzed by Particle Induced X-Ray Emission (PIXE, see Lucarelli et al., 2011 for details) at the LABEC-INFN facility in Florence (based on a 3 MV Tandetron accelerator, where an external beam set-up is fully dedicated to atmospheric aerosol studies. For daily samples we used a SIBATA HV-1000F high volume PM sampler (60 m^3h^{-1}) which excluded particles larger than 10 μm. this collected ~~obtained~~ 24 hr filter samples from 22nd March until 28th April (from 12:00 pm local time). Quartz fibre filters (ADVANTEC QR-100) were conditioned (30-40% relative humidity over 48h) and weighed before and after sampling to determine 24h PM_{10} concentrations by standard gravimetric procedures. Once the gravimetric determination was performed the filters were treated and analysed for the determination of the chemical composition of

PM_{10}. One quarter of each filter was acid digested ($HF:HNO_3:HClO_4$, with a mixture of 2.5:1.25:1.25 ml, kept at 90ºC in a Teflon reactor during 6h, driven to dryness and re-dissolved with 1.25 ml HNO_3 to make up a volume of 25 ml with water) for the chemical analysis using ICP-AES and ICP-MS. To assure the quality of the analytical procedure 5 mg of the NIST-1633b (fly ash) reference material loaded on a ¼ quartz micro-fibre filter were also analysed. Detection limit and accuracy of the techniques were estimated as 0.18 ngm^{-3} and 1-3% respectively for ICP-AES, and 0.007 ngm^{-3} and 0-7% respectively for ICP-MS. The detection limits for Zr and Hf are higher (0.05 ngm^{-3}). Another ¼ of each filter was water leached (6h at 60ºC, preceded by incubation in an ultrasound bath for 10 minutes, in 50 ml sealed PVC bottles) for the determination of soluble ion concentrations by ion chromatography (sulphate, nitrate and chloride) and ion selective electrode (ammonium), allowing an average detection limit for the analysed components of 25-30 ngm^{-3}. A portion (1.5 cm^2) of the remaining half of each filter was also used for the determination of organic and elemental carbon (OC and EC, respectively) by a thermal–optical transmission technique (Birch and Cary, 1996) using a Sunset Laboratory OC-EC Analyser with the EUSAAR-2 standard temperature programme. The accuracy of the equipment is in the rage of 5-10%, depending on the relative quantities of OC and EC on the filter, and the detection limit 0.2 μgm^{-3} for both OC and EC. The sum OC+EC is C_{total}. The OM+EC (organic matter plus elemental carbon) value was obtained after applying a 1.6 factor to the OC concentrations (Turpin et al., 2000).

SiO_2 and CO_3^{2-} were indirectly determined on the basis of empirical factors ($Al*1.89= Al_2O_3$, $3*Al_2O_3=SiO_2$ and $1.5*Ca+ 2.5*Mg=CO_3^{2-}$, see Querol et al., 2001). Blank field filters were used for every stock purchased for sampling and analysed in the same batches of their respective filter samples. The corresponding blank concentrations were subtracted from each sample.

A Positive Matrix Factorization (PMF, Paatero and Tapper, 1994) was performed on the two data matrices of concentrations and uncertainties of hourly Streaker samples values. This provides a reliable estimation of the main sources contributing to the measured PM by weighting each data point by its analytical uncertainty and solving the following equation:

$$x_{ij} = \sum_{h=1}^{p} g_{ih} f_{hj} + e_{ij} \qquad (1)$$

needs a bit more maybe?
How reliable?

The model uses the least squares method where the indices i, j and h refer to the number of samples, chemical components and factors respectively, while the matrices x, g and f refer to the concentration data, factor contribution (or factor scores) and factor profiles (or factor loading), respectively. The matrix e is the matrix of residuals defined as:

$$e_{ij} = x_{ij} - \sum_{h=1}^{p} g_{ih} f_{hj} \qquad (2)$$

The matrices g and f are found by minimizing the loss function Q defined as the sum of the squared residuals weighted by the uncertainty u_{ij} associated with the each data point:

$$Q = \sum_i \sum_j \left[\frac{e_{ij}}{u_{ij}} \right]^2 \qquad (3)$$

Individual estimates of the concentration errors were calculated following the methodology described by Amato et al. (2009). The uncertainty estimate provides a basis to separate species which retain a significant signal from the ones dominated by noise. This principle is based on the signal-to-noise S/N ratio described by Paatero and Hopke (2003). However, due to the sensibility of S/N to sporadic values much higher than the level of noise, the percentage of data above detection limit (ADL) was used as complementary criterion. Given the relatively low number of samples, species were selected to perform the source apportionment study. The selection was based on the Signal to Noise (S/N) ratio and % of data above detection limit criteria (Amato et al., 2009).

The transport pathways of air-masses into the Kumamoto area during the monitoring period were assessed using the HYSPLIT-model (Draxler and Rolph, 2003), with vertically modelled transport back-trajectories being calculated for 5 days at 750, 1500 and 2500 m a.s.l. In addition dust and sulphate maps forecasted by the Chemical Weather Forecasting System (CFORS) were obtained from the website of the National Institute for Environmental Studies (http://www-cfors.nies.go.jp/~cfors/) from 24th March onwards (before this date the system had been disrupted by the Great Eastern Japan earthquake on 11th March). CFORS numerically calculates distributions of Asian dust and anthropogenic sulphate aerosols every three hours, the results being uploaded on the website every day (Uno et al., 2003; Satake et al., 2004), and is widely referred to as a source of real-time information on movements of dust and pollution plumes over Asia. Finally, weather conditions (wind velocity and direction, precipitation, relative humidity and ambient temperature) were obtained from the Kumamoto Meteorological Observatory, located about 2 km west of the sampling site.

3 Results

Our PMF analysis of the Streaker coarse fraction ($PM_{2.5-10}$) data allows us to detect 4 main source factors (Fig. 2a) which are: 1. **Mineral dust** with major elements Si, Al, Ca, Fe, K, Mg and a range of trace elements that includes several metals such as Ti, Mn, Cu ; 2. **Metalliferous sodic aerosol**, accounting for 55% of Na and significant proportions of S, Mg, Ca, Cu, Zn and Sr; 3. **Fresh marine aerosol**, explaining almost 90% of Cl concentrations and including also Na and smaller amounts of Mg; 4. **ZnCu aerosol** attributed to traffic emissions and associated with mineral elements (Si, Al, Mg, Ca, K, Ti) related to dust resuspension processes.

See comments on the Figure

With regard to the fine aerosol fraction ($PM_{0.1-2.5}$) once again the best PMF solution is obtained with 4 factors (Fig. 2b), although with distinct differences from those of the coarser fraction: 1. **As- bearing Sulphatic aerosol**, dominated by S and As but also with smaller amounts of many other elements (K, Se, Sr, Ti, Mn, Fe, Zn) ; 2. **Metalliferous sodic aerosol**, which in this size fraction accounts for >80% of Na, associated with Se, Sr, Mg, Cu, Ca and S; 3. **Mineral dust**, including Al (Si not analysed), Ca, Fe, K, and Mg; 4. **Zn-Cu aerosol** again attributed mostly to traffic and explaining most of Zn and Cu (as seen in the coarse fraction), but also associated with Mn, K, Se, Fe, S and Sr suggesting a more mixed source for this very fine metalliferous component.

The chemical results for the 37 PM_{10} filter samples reveal considerable daily variation in PM concentrations. The full analyses are provided in Supplementary Information Appendix on Table S1 but a selected sample group representing the main chemical variation is provided in Table 1. The ICP-AES and MS database confirms predictions made by CFORS and HYSPLIT data and identifies two extended periods when transboundary sulphatic air pollution was most prominent (28th March-3rd April and 9-18th April), separated by a cleansing episode induced by the advection of oceanic air across Japan. Levels of nss-SO_4^{2-} rose to peaks exceeding 15 μgm^{-3} during the two pollution events (samples 290311, 150411 and 170411 on Table 1), but fell to a minimum of <2 μgm^{-3} during the intervening clean period (040411 and 190411 Table 1). The data also indicate the presence of elevated levels of mineral dust in several samples (e.g. 220311, 280311, 090411, 100411, 210411 Table 1), recorded by increased concentrations of typically "geological" major elements such as Al, Ca, Fe. Levels of Ti, a reliable tracer for mineral dust, rise above 55 ngm^{-3} during these *Kosa* events (Table 1).

The Streaker data are summarized in Fig. 3a-d and also clearly identify the two main pollution episodes (280311-030411 and 09-180411) separated by a phase of oceanic advection. Increased levels of fine sulphate (represented by S $PM_{0.1-2.5}$ on Fig. 3a) are typically accompanied by higher concentrations of the more toxic metallic elements (e.g. Pb, As on Fig. 3b). A somewhat contrasting pattern of fluctuations in the natural mineral dust component is represented by concentrations of Al and Ca (hourly Streaker data) plotted in Fig. 3c, revealing a series of transient peaks of these crustal elements as waves of Gobi dust crossed Kyushu during the 6-week sampling period. With reference to Fig. 3 we now consider these air quality events in more detail by subdividing the results from the sampling period into five distinct phases.

3.1 Phase 1: 17-27 March

The first 10 days of the Streaker campaign (and 6 days of the filter sampling campaign) were characterized by NW winds feeding in transient and relatively dilute waves of aerosols from the Asian mainland (both Gobi desert dust and Chinese industrial pollutants) clockwise around anticyclones moving east from central China. Meteorological conditions did not favour the stagnation and concentration of anthropogenic pollutants in central China so the amount of atmospheric particulates entering Japan was not exceptional and PM levels stayed below 40 μgm^{-3}, with both nss-SO_4^{2-} and NO_3^- concentrations being confined to a narrow range (3-6 μgm^{-3}). The amounts of mineral dust fluctuated between 5-14 μgm^{-3} depending on the timing of the arrival of Gobi intrusions. Whereas the first desert dust event recorded (19th March) was relatively uncontaminated, later peaks (filter samples 220311, 240311 Table 1) coincide with peaks in $S_{0.1-2.5}$ (Fig. 3a, c) and so show elevated concentrations of both crustal and SIC (SO_4^{2-}+NO_3^-+ NH_4^+>10 μngm^{-3}). The cleanest conditions were produced by rainfall (afternoon of 20th March), and five short-lived NaCl hourly peaks occurred during periods of increased wind speed blowing sea spray into the island (Fig. 3d). The passing waves of aerosols arriving into Kyushu from offshore were interspersed with periods of light winds and low temperatures when traffic-derived local pollutants in Kumamoto took precedence over transboundary PM intrusions. Such conditions favoured high NO_3^- relative to SO_4^{2-} and concentration spikes in several metals (Cr, Co, Ni, Cu, Zn, Sb) and C which we attribute to traffic emissions (the best example being 240311 Table 1).

3.2 Phase 2: 28 March – 3 April

The air quality data from this period track a major sulphatic transboundary intrusion event driven by an anticyclone initially persisting in east central China then moving east, dragging the pollution plume oceanward to cover Japan and much of the NW Pacific (Fig. 1). Kyushu was constantly visited by this vast, recirculating plume of dispersing pollutants as it waxed and waned across the region, raising peak daily average PM_{10} concentrations at Kumamoto to 66 μgm^{-3} (Sample 290311 Table 1). Most of the increase in ambient PM is due to an important sharp rise in SIC (from <10 μgm^{-3} to >20 μgm^{-3}), but on some days there were also increases in Gobi desert dust as cold high level air sourced from Mongolia raised daily mineral dust levels back above 10 μgm^{-3} (Fig. 3c, sample 280311 Table 1). Streaker data demonstrate these *Kosa* peaks to have been highly transient in nature, rising and falling over half a day or less (Fig. 3c). In contrast, metalliferous sulphatic pollutants build up more gradually to successive peaks which tend to arrive slightly later than the "mineral dust" peak, and linger in the atmosphere as fine grained, atmospherically persistent particles (Fig. 3b). Another chemical characteristic of this phase is relatively high levels of NO_3^- which over the first four days rise above 8.0 μgm^{-3}. Such concentrations are attributed to the mixing of cold, humid air with industrial pollutants, inhibiting thermal dissociation of ammonium nitrate and so favouring high levels of particulate NH_4NO_3 which attained a campaign maximum on 29-30th March (see NO_3^- and NH_4^+ levels of sample 290311 on Table 1) when rainy conditions in Kumamoto were accompanied by poor visibility and average temperatures remained below 10°C. From the following day onwards during the campaign average daily temperatures were to rise into double figures and such elevated levels of NO_3^- were not recorded again.

use the equation or name not both together

3.3 Phase 3: 3-8 April

There is a complete change in air quality as winds rotate clockwise away from the Asian mainland, sourcing firstly from the NE (Sea of Japan: 3-5th April) then progressively from the SE and S (Pacific Ocean: 6-8th April). The advection of marine air across Kyushu results in a series of NaCl peaks recorded by the Streaker data, building up eventually to the most prominent in response to the influence of a warm, rapidly moving airstream from the open ocean to the south (Fig. 3d, peak on 8th April; sample 080411 Table 1). Under these conditions of cleansing marine air advection there is a fall in ambient PM_{10} levels to around 20 μgm^{-3} (samples 060411 and 070411, Table S1), and levels of contaminants C_t, NO_3^-, SO_4^{2-}, NH_4^+, Sc, V, Ni, Cu, As, Cd, Sn, Pb, and Bi all decline to a campaign minimum. In fact, by the end of this phase, concentrations of the most toxic elements such

does the rainfall also increase during this period?

as Pb, Bi, As, and Cd are a mere 5-8% of their maxima reached during Phase 2 the previous week. Ambient levels of mineral dust are subdued to within the narrow range of 5-8 μgm^{-3}, with the exception of a transient peak on 7th April (Fig. 3c) which we attribute to a local resuspension event under unusually strong afternoon winds (6 ms^{-1}).

3.4 Phase 4: 8-19 April

? 'Joined' ?

The next phase begins as a repeat performance of Phase 2, with anticyclonic conditions once again favouring atmospheric stagnation and the concentration of anthropogenic pollutants over a wide area across the Chinese central lowlands from Wuhan to Shanghai and Qingdao. This pollution plume is invaded from the NW by a Gobi desert dust intrusion and both masses move eastward into the Yellow Sea. Over the first 3 days (8-10th April) the anticyclone moves east across Japan, replacing initially rainy overcast conditions with dry bright hazy conditions under light winds as the contaminating transboundary pollution plume (both dust and SIC) rotates clockwise around the eastward drifting anticyclone. The southern edge of the SO_4^{2-} plume, still relatively dilute, arrives in Kyushu on the afternoon of 8th April (Fig. 3a), followed that evening by Gobi dust which peaks the following midday (Fig. 3c). This is the biggest *Kosa* event in the campaign (sample 090411 Table 1, 45 $\mu gPM_{10}m^{-3}$) and is followed by further mineral dust peaks over the next two days (Fig. 3c) as the dust intrusion recirculates over Kyushu producing campaign maxima in Ca, Al, Fe, K, Mg, Li, Be, Sc, Ti, Mn, Co, Rb, Sr, REE, Ta, U (samples 090411, 100411 Table 1). Sulphur $PM_{0.1-2.5}$ recorded by the Streaker also peaks at midday 9th April but then does not decline significantly (unlike the mineral dust), rising later to a final peak on 11th April (Fig. 3a) in response to a new wave of pollutants brought in by a second anticyclone once again moving eastward from central China. By this time virtually the whole of Japan has been covered with the mixed sulphatic+mineral dust plume.

then it is a single mass ?

form

The effect of the new anticyclonic ridge building out from central China was not only to add new contaminants to the system, but also to disperse the existing plume even more widely over the W Pacific region, creating a vast recirculating mass of contaminants, some of which arrive back into their original source area on the mainland. Kyushu lay in a central but relatively dilute part of this huge pollution plume, experiencing only minor insults to air quality (around 12th April, Fig. 3) until a more concentrated band of the same mixed aerosol mass was pushed back into the island. Under these conditions on 13-14th

April there was a repeat of events 3 days earlier, with mineral dust and metalliferous $S_{0.1-2.5}$ PM attaining new peaks (Figs. 3a, c).

The final part of this prolonged regional pollution event was especially interesting. Whereas all previous arrivals of SIC contaminants had travelled out from China via a NW corridor typically involving transport over the Yellow Sea, by 15th April a concentrated wave of industrial pollutants was travelling directly east from the Shanghai coast into western Japan. This fresh new wave of transboundary aerosols produced the most pronounced pollution event during the campaign (18 $\mu g SO_4^{2-} m^{-3}$). Beginning with the arrival around midnight on 15th April of a brief peak of aluminous dust accompanied by SIC (Figs. 3a, c), levels of anthropogenic contaminants were to hit new maxima on the 16th and 17th April (Fig. 3b; samples 150411, 160411, 170411 Table 1). The trace element content accompanying this sulphatic and carbonaceous aerosol intrusion is again very metalliferous (high V, Cd, Sn, Bi, K, Pb, Sb, As, Zn, W) but the chemical mix is subtly different from those recorded previously, with unusually high levels of total carbon, V, Cd, Sn and differences in element ratios (e.g. higher As/Se). This multiple pollution event was finally terminated on the evening of 18th April with the arrival of strong, clean NNW winds carrying enough sea spray to mark a marine event (Fig. 3d).

Any signal in the S? The more northern Chinese coals ~~than~~ tend to have more pyrite than northern coals?

3.5 Phase 5: 19-28 April

The northerly advection event which swept the Phase 4 pollution plume south of Japan during 18-19th April was initially accompanied by an uncontaminated *Kosa* event which briefly raised crustal dust levels as SIC concentrations continued to fall rapidly (compare Figs. 3a and 3c, 18th April). The following day, still dominated by a strong northerly Russian airflow moving into Kyushu via the Korean Peninsula and Sea of Japan, provided the cleanest 24h filter of the entire sampling campaign, with PM_{10} levels dropping to 18.6 $\mu g m^{-3}$, mineral dust to 3 $\mu g m^{-3}$ and SIC to 4 $\mu g m^{-3}$ (sample 190411 Table 1). However this rapid and thorough atmospheric cleansing event provided only brief respite from the Chinese pollution plume, which continued to recirculate widely across the NW Pacific and returned into Japan on 20th April. For the remainder of the campaign this diluted but persistent SO_4^{2-} haze recirculated over Japan, occasionally supplemented by influxes of fresh mainland contaminants and Gobi dust to produce several minor $S_{0.1-2.5}$ and $Al_{2.5-10}$ peaks (Fig. 3a and 3c; sample 240411 Table 1). Comparison between the coarser and finer PM fractions in the Streaker data indicate an increase in the coarser sulphate particles

($S_{PM0.1-2.5/PM2.5-10}$ drops from 20.4 in Phase 4 to 9.9 in Phase 5), suggesting a relative coarsening by coagulation and chemical interaction of PM with gaseous precursors with time as the regional pollution plume ages and persists across the NW Pacific region (Fig. 3a).

4 Discussion and conclusions

The chemical data summarized in this paper allow us to view both hourly and daily fluctuations in transboundary aerosols affecting Japanese ambient air quality over a 6-week period in spring, and provide a clearer idea of the reality of what people are inhaling at that time of the year. The PMF analysis of Streaker hourly data confirm that natural PM dominate in the coarser PM fraction ($PM_{2.5-10}$), with continental mineral dust dominant over fresh marine aerosol. In the finer fraction ($PM_{0.1-2.5}$) however the mineral dust is much less abundant and instead the dominant component is As-bearing sulphatic aerosol. The metalliferous sodic PM component recognised in both size fractions is suggested to represent dechlorinated, sulphate-enriched aged sea salt aerosols contaminated by industrial emissions during long-distance transport.

No extreme *Kosa* events (when average daily PM_{10} concentrations in Japan can rise dramatically to well above 100 μgm^{-3}) were recorded during the campaign, but instead our sampling interval was typical of what these days may be considered normal springtime conditions. Under such conditions prevailing NW winds bring frequent but normally brief intrusions of Gobi dust into western Japan so that during the combined 4-week period of phases 1, 2 and 5 our data recorded nine such "natural" events when concentrations of Al exceeded 1 μgm^{-3} (Fig. 3c) for a few hours. A notably heavier loading of mineral dust occurred during the pollution episode of Phase 4, but even here the peaks remained highly transient, with concentrations of Al rising from around 1 $\mu g/m^3$ to double or triple over 2 or 3 hours but then falling back equally rapidly. In contrast the anthropogenic component of suspended particulate matter in the atmosphere usually builds up more slowly and does not fully decline as rapidly as the mineral dust. Once $S_{0.1-2.5}$ levels rose above 2 μgm^{-3} during the pollution episodes of Phases 2 and 4 they stayed high, reflecting the atmospherically persistent nature of this extremely fine sulphatic PM. The same behaviour can be seen in the metalliferous components, well displayed by Pb, Zn, Sn and As on Figs. 3a-b which consistently correlate more with the sulphatic component than with the natural mineral dust.

It is clear that transboundary aerosol intrusions arriving into Japan are chemically inhomogeneous. As we have observed in our precursor pilot study of *Kosa* events in Kyushu, some waves of Gobi dust are more calcareous than others, presumably depending on their geological source area (Yuan et al., 2008; Zhang et al., 2005; Shao et al., 2008; Moreno et al., 2012). The Streaker data reinforce this observation of natural chemical variables in transboundary events, with later mineral dust peaks in phases 4 and 5 registering as more aluminous than earlier, more calcareous ones (Fig. 3c). Furthermore, our data reveal distinct differences in the chemical signature of the Asiatic mainland pollution plume, even after a journey of around 1000 km or more from source. The best example is provided by the unusually high levels of SO_4^{2-}, V, Cd, Sn, Bi, Cu, As, Sb, and Pb in response to the arrival of pollution directly from East China into Kyushu on 15th April. Yet another confounding factor for those trying to determine the possible health effects of transboundary aerosols is the way peak concentration arrivals of mineral dust are commonly not synchronous with anthropogenic pollution peaks. A good example of this is provided by Phase 4 when the initial arrival of a *Kosa* PM wave was accompanied by a much slower buildup to a sulphate peak (Figs. 3a and c). Indeed, the high levels of natural dust at the beginning of Phase 4 contrast greatly with the later peaks in anthropogenic contaminants as the sulphatic plume was repeatedly recharged by mainland-sourced pollution without any additional influence of Gobi desert dust. Finally, while still on the theme of chemical variation within the East Asian pollution plume, our data show considerable differences in ambient PM nitrate concentration (from 1 to 16 μgm^{-3}), depending not just on local *versus* exotic sources but also on temperature controlling the volatility of atmospheric ammonium nitrate.

The magnitude of the loss in air quality over Japan due to the 21st century spread of the mainland Asiatic pollution plume is emphasized by our Phase 3 record of 5 days when winds brought air from the oceanic rather than continental sector. As the origin of these winds crossing SW Japan rotated clockwise from north to east to south we see proof of how little regional industrial air pollution these days originates from the Japanese archipelago. The arrival of contaminated air masses from mainland Asia is forecasted daily by the Chemical Weather Forecasting System (CFORS) which numerically calculates distributions of Asian dust and anthropogenic sulphate aerosols every three hours, the results being uploaded on the website every day (http://www-cfors.nies.go.jp/~cfors/). Average levels of anthropogenic pollutants elements fall

395 abruptly, in some cases by >90%, as the continental source is removed. This is especially
396 true of the most undesirable pollutants: Pb from >60 to 3 ngm^{-3}, As from 6 to 0.3 ngm^{-3}, Cd
397 from 1.1 to 0.09 ngm^{-3}. Things, of course, were not always this way, with extreme levels of
398 Japanese air pollution accompanying rapid industrialization in the mid 1950s to mid-
399 1960s, leading to the introduction of the Basic Law for Environmental Pollution Control
400 in 1967 (Kawamoto et al., 2011). The modern problem in Japan thus has to be placed in
401 perspective, and is clearly less severe than impacts on air quality in many parts of urban
402 China (Kan et al., 2007; Okuda et al., 2008; Zhao et al., 2008; Saikawa et al., 2009; Zheng
403 et al., 2011). However, even given the more dilute character of the transboundary plumes
404 reaching neighbouring receptor countries, their atmospheric persistence and highly
405 respirable nature create reasonable cause for concern. Much of this concern has focussed
406 more on the pulmonary toxicity and corresponding acute effects of PM inhalation,
407 especially on asthmatic patients (e.g. Ichinose et al., 2005; Ueda et al., 2010; Watanabe et
408 al., 2010), or on the potential transport of active bioaerosols between countries (e.g. Chen
409 et al., 2010). However, a greater health problem is more likely to be related to premature
410 deaths from cardiovascular and respiratory diseases resulting from long-term exposure to
411 elevated levels of atmospherically persistent, respirable, metalliferous PM (Chan et al.,
412 2008; Liu et al., 2009). Our 6-week continuous database from Kumamoto demonstrates
413 the constantly changing chemical complexity of this pernicious problem.
414

415 **Acknowledgments**

416 This work was supported by the Invitation Fellowship Program for Research of the Japan
417 Society for the Promotion of Science (No. 11019, TM), by the Generalitat de Catalunya
418 (CUR- DIUE: BE-DGR 2010, TM), and partly by the Grant-in-Aid for Scientific Research
419 (No. 17684026, TK). TK also thanks Drs. D. Zhang and T. Nagatani for cooperation with
420 air monitoring in the Kumamoto area.
421
422

423 **References**

424 Amato, F., Pandolfi, M., Escrig, A., Querol, X., Alastuey, A., Pey, J., Perez, N. and Hopke, P.K.:
425 Quantifying road dust resuspension in urban environment by multilinear engine: a comparison
426 with PMF2. Atmos. Environ. 43, 2770-2780, 2009.

427 Birch, ME. and Cary, RA.: Elemental carbon based method for monitoring occupational exposures
428 to particulate diesel exhaust. Aerosol Sci. and Technol 25, 221-241, 1996.

429 Chan, C. and Yao, X.: Air pollution in mega cities in China. Atmos. Environ. 42, 1-42, 2008.

430 Chan, CC., Chuang, KJ., Chen, WJ., Chang, WT., Lee, CT. and Peng, CM.: Increasing
431 cardiopulmonary emergency visits by long-range transported Asian dust storms in Taiwan.
432 Environ. Res. 106, 393-400, 2008.

433 Chen, C., Tsa, F., Lin, C., Yang, C., Chan, C., Young, C. and Lee, C.: Ambient influenza and
434 avian influenza virus during dust storm days and background days. Environ. Health Perspect. 118,
435 1211-1216, 2010.

436 Chung, YS. and Kim, HS.: Observations of massive air-pollution transport and associated air
437 quality in the Yellow Sea region. Air Quality and Atmo.s Health 1, 69-79, 2008.

438 Draxler, RR. and Rolph, GD.:HYSPLIT (HYbridSingle-Particle Lagrangian Integrated Trajectory)
439 Model Access via NOAA ARL READY Website. NOAA Air Resources Laboratory, SilverSpring,
440 MD. http://www.arl.noaa.gov/ready/hysplit4.html. 2003.

441 Fairlie, TD., Jacob, DJ., Dibb, JE., Alexander, B., Avery, MA., van Donkelaar, A. and Zhang, L.:
442 Impact of mineral dust on nitrate, sulphate, and ozone in transpacific Asian pollution plumes.
443 Atmos. Chem. Phys. 10, 3999-4012, 2010.

444 Guo, J., Rahn, K. and Zhuang, G.: A mechanism for the increase of pollution elements in dust
445 storms in Beijing. Atmos. Environ. 38, 855-862, 2004.

446 Ianniello, A., Spataro, F., Esposito, G., Allegrini, I., Hu, M. and Zhu, T.: Chemical characteristics
447 of inorganic ammonium salts in PM2.5 in the atmosphere of Beijing (China). Atmos. Chem. Phys.
448 11, 10803–10822, 2011.

449 Ichinose, T., Nishikawa, M., Takano, H., Sera, N., Sadakane, K., Mori, I., et al.: Pulmonary
450 toxicity induced by intratracheal instillation of Asian yellow dust (Kosa) in mice. Environ.
451 Toxicol. Pharmacol. 20, 48-56, 2005.

452 Kan, HD., London, S., Chen, G., Zhang, Y., Song, G., Zhao, N., et al.: Differentiating the effects
453 of the fine and coarse particles on daily mortality in Shanghai, China. Environ. Int. 33, 376-384,
454 2007.

455 Kawamoto, T., Pham, TT., Matsuda, T., Oyama, T., Tanaka, M., Yu, HS. and Uchiyama, I.:
456 Historical review on development of environmental quality standards and guideline values for air
457 pollutants in Japan. Int. J. Hygiene Environ. Health 214, 296-304, 2011.

Lasserre, F., Cautenet, G., Bouet, C., Dong, X., Kim, YJ., Sugimoto, N., et al.: A model tool for assessing real-time mixing of mineral and anthropogenic pollutants in east Asia: a case study of April 2005. Atmos. Chem. Phys. 8, 3603-3622, 2008.

Liu, J. and Mauzerall, DL.: Potential influence of inter-continental transport of sulfate aerosols on air quality. Environmental Research Letters (2) 045029, doi:10.1088/1748-9326/1082/1084/045029. 2007.

Liu, J., Mauzerall, DL. and Horowitz, LW.: Source-receptor relationships between East Asian sulphur dioxide emissions and Northern Hemisphere sulphate concentrations. Atmos. Chem. Phys. 8, 3721-3733, 2008.

Liu, J., Mauzerall, DL. and Horowitz, LW.: Evaluating inter-continental transport of fine aerosols: (2) Global health impact. Atmos. Environ. 43, 4339-4347, 2009.

Lucarelli, F., Nava, S., Calzolai, G., Chiari, M., Udisti, R. and Marino, F.: Is PIXE still a useful technique for the analysis of atmospheric aerosols? The LABEC experience. X-Ray Spectrometry 40, 162–167, 2011.

Ma, C., Tohno, S., Kasashara, M.and Hayakawa, S.: The nature of individual solid particles retained in size-resolved raindrops fallen in Asian dust store event during ACE-Asia. Atmos. Environ. 38, 2951-2964, 2004.

Moreno, T., Kojima, T., Querol, X., Alastuey, A., Amato, F. and Gibbons, W.: Natural *versus* anthropogenic inhalable aerosol chemistry of transboundary East Asian atmospheric outflows into western Japan. Sci. Tot. Environ. 424, 182-192, 2012.

Ohara, T., Akimoto, H., Kurokawa, J., Horii, N., Yamaji, K., Yan, X. and Hayasaka, T.: An Asian emission inventory of anthropogenic emission sources from the period 1980-2020. Atmos. Chem. Phys. 7, 4419-4444, 2007.

Okuda, T., Katsuno, M., Naoi, D., Nakao, S., Tanaka, S., He, K., et al.: Trends in hazardous trace metal concentrations in aerosols collected in Beijing, China from 2001 to 2006. Chemosphere 72, 917-924, 2008.

Onishi, K., Kurosaki, Y., Otani, S., Yoshida, A., Sugimoto, and Kurozawa, Y.: Atmospheric transport route determines components of Asian dust and health effects in Japan. Atmospheric Environment doi:10.1016/j.atmosenv.2011.12.018.

Paatero, P. and Hopke, P.K.: Discarding or downweighting high-noise variables in factor analytic models. Analytica Chimica Acta 490, 277-289, 2003.

Paatero, P. and Tapper, U.: Positive matrix factorization: a non-negative factor model with optimal utilization of error estimates of data values. Environmetrics 5, 111-126, 1994.

Prospero, JM., Savoir, DL. and Arimoto, R.: Long-term record of nss-sulfate and nitrate in aerosols on Midway Island, 1981-2000: evidence of increased (now decreasing?) anthropogenic emissions from Asia. Journal of Geophysical Research 108, doi:10.1029/2001JD001524. 2003.

Querol, X., Alastuey, A., Rodríguez, S., Plana, F., Ruiz, CR., Cots, N., et al.: PM10 and PM2.5 source apportionment in the Barcelona Metropolitan Area, Catalonia, Spain. Atmos. Environ. 35/36, 6407-6419, 2001.

Saikawa, E., Naik, V., Horowitz, L., Liu, J. and Mauzerall, D.: Present and potential future contributions of sulphate, black & organic carbon aerosols from China to global air quality, premature mortality and radiative forcing. Atmos Environ 43, 2814-2822, 2009.

Satake, S., Uno, I., Takemura, T., Carmichael, G., Tang, Y., Streets, D., et al.: Characteristics of Asian aerosol transport simulated with a regional-scale chemical transport model during the ACE-Asia observation. Journal of Geophysical Research 109:D19S22. doi:10.1029/2003JD003997. 2004.

Shao, LY., Li, WJ., Xiao, ZH. and Sun, ZQ.: The mineralogy and possible sources of spring dust particles over Beijing. Advances in Atmos. Sci. 25, 395–403, 2008.

Takahashi, H., Naoe, H., Igarashi, Y., Inomata, Y. and Sugimoto, N.: Aerosol concentrations observed at Mt. Haruna, Japan, in relation to long-range transport of Asian mineral dust aerosols. Atmos. Environ. 44, 4638-4644, 2010.

Turpin, BJ., Saxena, P., Andrews, E., 2000. Measuring and simulating particulate organics in the atmosphere: problems and prospects. Atmospheric Environment 34, 2983–3013.

Ueda, K., Nitta, H.and Odajima, H.: The effects of weather, air pollutants, and Asian dust on hospitalization for asthma in Fukuoka. Environ. Health Preventive Med. 15, 350-357, 2010.

Uno, I., Carmichael, G., Streets, D., Tang, Y., Yienger, J., Satake, S., et al.: Regional chemical weather forecasting system CFORS: Model descriptions and analysis of surface observations at Japanese island stations during the ACE-Asia experiment. Journal of Geophysical Research 108(D23):8668, doi:10.1029/2002JD002845. 2003.

Uno, I., Satake, S., Carmichael, G., Tang, Y., Wang, Z., Takemura, T., et al.: Numerical study of Asian dust transport during the springtime of 2001 simulated with the chemical weather forecasting system (CFORS) model. Journal of Geophysical Research 109:D19S24. doi:10.1029/2003JD004222. 2004.

Wang, X., Dong, Z., Zhang, J.and Liu, L.: Modern dust storms in China: an overview. J. Arid Environ. 58, 559-574, 2004.

Watanabe, M., Yamasaki, A., Burioka, N., Kurai, J., Moneda, K., Yoshida, A., et al., 2010. Correlation between Asian dust storms and worsening asthma in western Japan. Allergology International doi: 10.23327allergolint.10-OA-0239.

Yuan, H., Zhuang, G., Li, J., Wang, Z. and Li, J.: Mixing of mineral with pollution aerosols in dust season in Beijing: revealed by source apportionment study. Atmos. Environ. 42, 2141-2157, 2008.

Zhang, W., Zhuang, G., Huang, K., Li, J., Zhang, R., Wang, Q., et al.: Mixing and transformation of Asian dust with pollution in the two dust storms over the northern China in 2006. Atmos. Environ. 44, 3394-3403, 2010.

Zhang, XY., Wang, YQ. Wang, D. Gong, SL. Arimoto, R., Mao, LJ. and Li, J.: Characterization and sources of regional-scale transported carbonaceous and dust aerosols from different pathways in coastal and sandy land areas of China. Journal of Geophysical Research-Part D-Atmospheres 110:doi: 10.1029/2004JD005457. 2005.

Zhao, Y., Wang, S., Duan, L., Cao, P. and Hao, J.: Primary air pollutant emissions of coal-firepower plants in China: current status and future prediction. Atmos. Environ. 42, 8442-8452, 2008.

Zheng, M., Wang, F., Hagler, GSW., Hou, X., Bergin, M., Cheng, Y., Salmon, L.G., , Schauer, J., Louie, P., Zeng, L. and Zhang, Y.: Sources of excess urban carbonaceous aerosol in the Pearl River Delta Region, China. Atmos. Environ. 45, 1175-1182, 2011.

541 **Figure and table captions**

542

543 Figure 1. Location map overviewing the area affected by the transboundary expulsion of
544 anthropogenic aerosols from China into the NW pacific region. Arrows depict typical
545 atmospheric circulation patterns driving the pollution eastward out from the mainland, in
546 this case by an anticyclone centred near Shanghai during the sampling period at the end of
547 March 2011 (based on CFORS, a database widely referred to as a source of real-time
548 information on movements of dust and pollution plumes over Asia: http://www-
549 cfors.nies.go.jp/~cfors/). The monitoring site in Kumamoto lies on the island of Kyushu in
550 SW Japan, in the area most frequently visited by transboundary PM outflows from the
551 mainland. The main source areas of springtime desert dust intrusions into the area are also
552 shown (Wang et al., 2004).

553

554 Figure 2. Chemical profile for each factor identified by Positive Matrix Factorization
555 (PMF) for hourly Streaker samples showing concentration histograms and the explained
556 variation for each element.

557

558 Figure 3. Hourly selected elemental concentrations (ng/m^3) obtained with the Streaker
559 sampler for the five air quality phases identified during the monitoring campaign, with
560 coloured bands highlighting main episodes of continental pollution and advection of salty
561 marine air across Kumamoto. Fig. **3a** shows both coarse ($PM_{2.5-10}$) and fine ($PM_{0.1-2.5}$)
562 sulphatic aerosol intrusions. Whereas the finer fraction of these aerosols is always
563 dominant (compare different scales), there is a clear tendency towards coarsening as the
564 pollution plume introduced during Phase 4 is briefly forced south by northerly winds but
565 brought back to age and recirculate over Japan during Phase 5. Fig. **3b** uses Pb and As
566 hourly concentrations to illustrate how toxic metallic aerosols accompany the sulphatic
567 intrusions. Fig. **3c** uses hourly concentrations of Al and Ca to reveal the rise and fall of
568 Gobi desert PM introduced by NW winds crossing NE China and therefore usually mixed
569 to some extent with anthropogenic pollutants. Fig **3d** uses hourly concentrations of Na and
570 Cl to identify marine aerosol episodes, with Phase 1 recording several transient periods of
571 strong NW winds accompanied by Gobi dust and sea spray sourced from the Yellow Sea,
572 whereas Phase 3 shows a prolonged period of atmospheric cleansing under non-
573 continental winds sourcing initially from the Sea of Japan and then from the Pacific
574 Ocean.

575

576

577 Table 1. Daily, average, maximum, and standard deviation values for elemental
578 concentrations analysed in selected PM_{10} gravimetric filters collected in Kumamoto
579 March-April 2010 (see text for details), including average values for the full dataset from
580 22 March to 28 April. Each sample bears the date when 24-hour sampling started at
581 midday and therefore includes the first half of the following day. PM and major element
582 concentrations are in $\mu g/m^3$, trace elemental concentrations in ng/m^3. Mineral=CO_3^{2-}
583 $+SiO_2+Al_2O_3+Ca+Fe+K+Mg$; OM+EC= Organic matter + elemental carbon;
584 SIC=NH_4^++NO_3^-+SO_4^{2-}; Marine=Na+Cl.

585

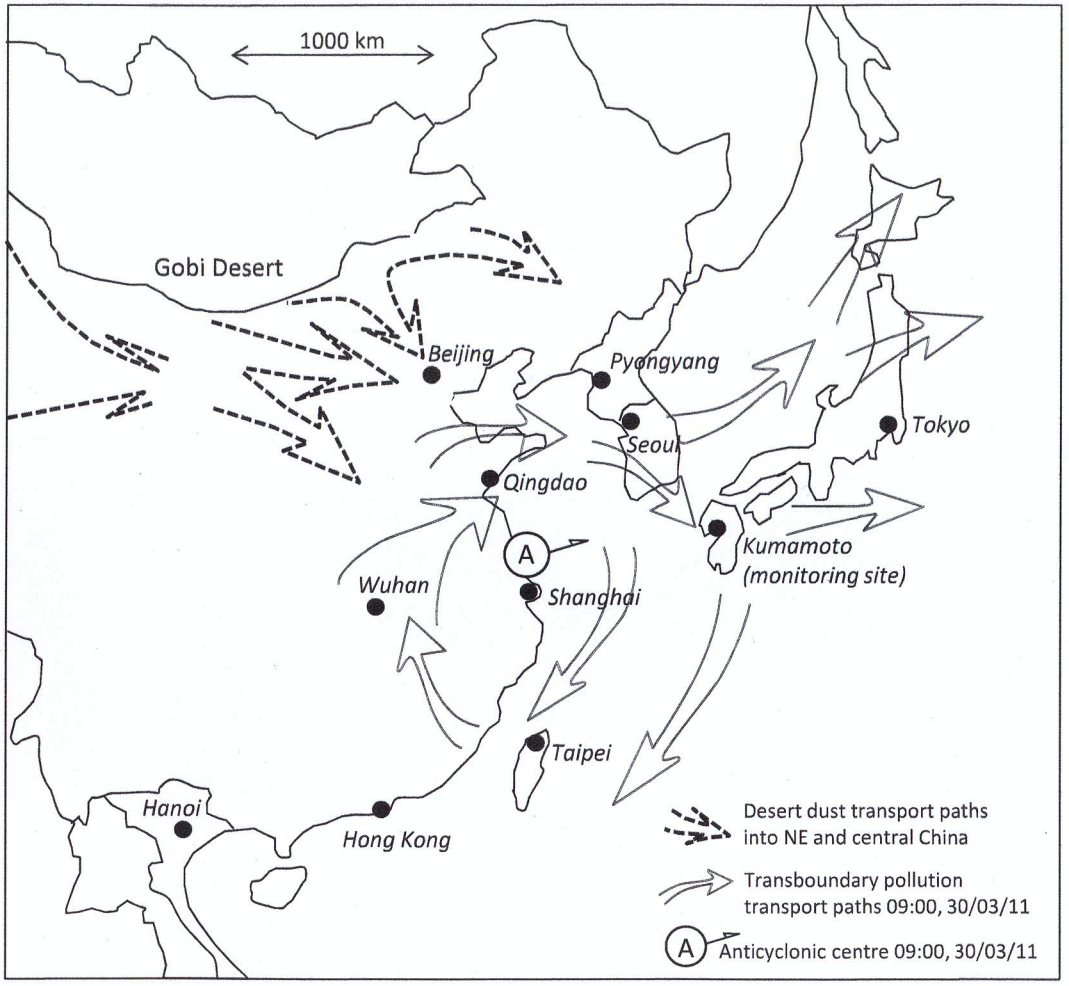

A bit too abstract? Could the land masses have a gentle shading?

Fig. 1

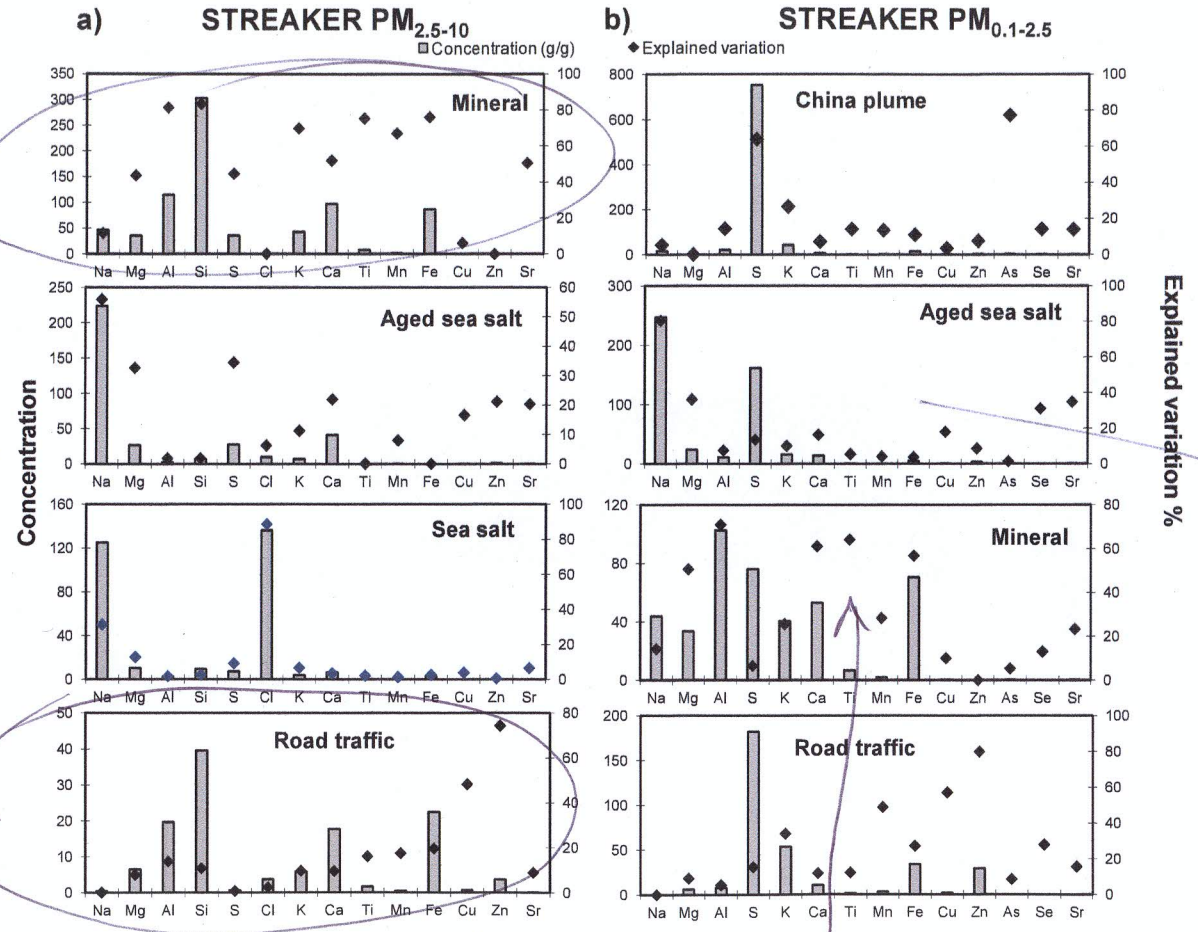

look very similar?

no value for chlorine?

mineral / road traffic mixture?

Fig. 2

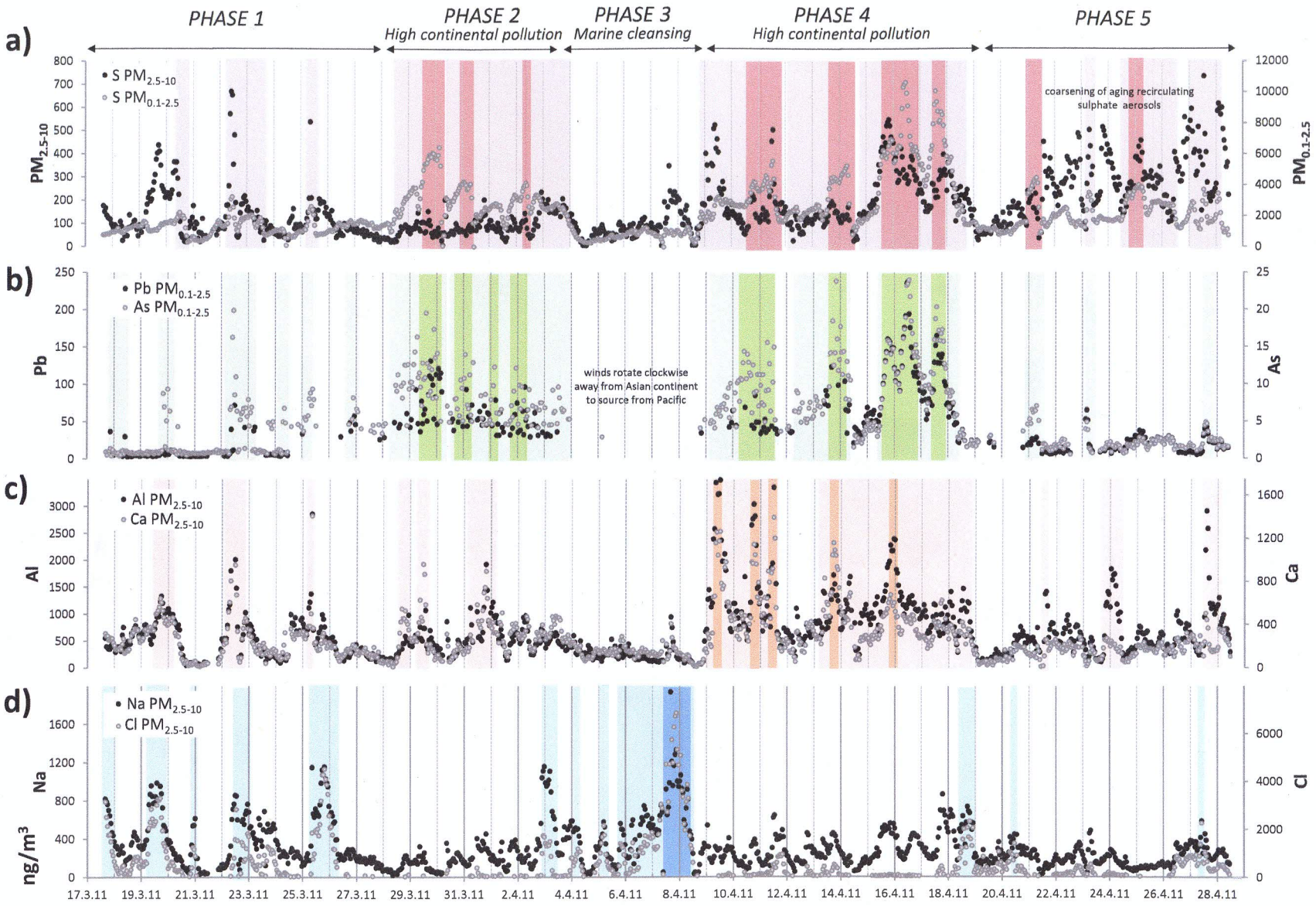
PHASE 1
PHASE 2
High continental pollution
PHASE 3
Marine cleansing
PHASE 4
High continental pollution
PHASE 5
a)
S PM2.5-10
S PM0.1-2.5
PM2.5-10
PM0.1-2.5
coarsening of aging recirculating sulphate aerosols
b)
Pb PM0.1-2.5
As PM0.1-2.5
Pb
As
winds rotate clockwise away from Asian continent to source from Pacific
c)
Al PM2.5-10
Ca PM2.5-10
Al
Ca
d)
Na PM2.5-10
Cl PM2.5-10
Na
Cl
ng/m3
17.3.11
19.3.11
21.3.11
23.3.11
25.3.11
27.3.11
29.3.11
31.3.11
2.4.11
4.4.11
6.4.11
8.4.11
10.4.11
12.4.11
14.4.11
16.4.11
18.4.11
20.4.11
22.4.11
24.4.11
26.4.11
28.4.11

Fig. 3

Date	220311	230311	240311	280311	290311	040411	080411	090411	100411	150411	160411	170411	190411	210411	240411	average	max	std. dev
µg/m³																		
PM_{10}	39.65	22.94	36.39	47.69	65.73	22.94	27.72	45.07	52.34	54.86	63.99	54.73	18.60	47.58	36.34	37.62	65.73	12.41
OM+EC	7.03	6.93	11.23	11.03	11.78	4.53	4.26	8.72	10.42	9.01	18.16	13.40	5.13	11.67	9.05	8.96	18.16	3.14
OC	3.99	3.96	6.13	6.24	6.80	2.60	2.49	5.41	6.14	5.17	10.33	7.88	2.78	6.78	5.20	5.12	10.33	1.81
EC	0.84	0.54	1.21	1.02	0.76	0.42	0.39	0.52	0.80	0.71	1.30	0.76	0.55	0.89	0.55	0.72	1.30	0.24
$CO_3^=$	2.19	0.86	1.65	1.83	1.00	0.94	1.13	2.41	2.11	1.25	1.44	1.33	0.60	1.89	0.45	1.20	2.41	0.47
SiO_2	6.78	2.44	4.97	5.52	3.73	4.66	4.25	8.33	7.24	3.60	4.43	4.15	1.40	8.46	1.38	4.10	8.46	1.64
Al_2O_3	2.26	0.81	1.66	1.84	1.24	1.55	1.42	2.78	2.41	1.20	1.48	1.38	0.47	2.82	0.46	1.37	2.82	0.55
Ca	0.79	0.30	0.68	0.80	0.44	0.39	0.36	0.85	0.80	0.42	0.48	0.45	0.20	0.77	0.17	0.45	0.85	0.18
Fe	0.81	0.32	0.68	0.77	0.59	0.61	0.49	0.99	0.94	0.50	0.59	0.55	0.19	0.90	0.24	0.52	0.99	0.19
K	0.54	0.23	0.37	0.53	0.52	0.19	0.33	0.65	0.70	0.55	0.67	0.59	0.13	0.55	0.37	0.40	0.70	0.17
Na	0.61	0.38	0.32	0.36	0.25	0.40	0.30	0.51	0.46	0.88	1.09	1.02	0.61	0.61	0.25	0.55	1.11	0.25
Mg	0.40	0.16	0.25	0.25	0.14	0.14	0.23	0.46	0.37	0.25	0.29	0.26	0.12	0.29	0.08	0.21	0.48	0.08
Cl	0.80	0.17	0.47	0.36	0.79	1.22	n.a.	0.19	0.10	0.43	0.65	0.64	0.47	0.21	0.38	0.48	1.22	0.28
NO_3^-	4.40	3.87	5.98	8.13	16.12	1.77	1.31	4.21	4.58	6.15	4.42	3.74	2.02	2.91	5.03	4.58	16.12	2.92
$SO_4^=$	5.10	3.15	3.73	9.21	16.56	1.90	4.06	4.57	7.03	18.00	11.21	16.99	1.97	7.25	10.46	6.98	18.00	4.10
nss-$SO_4^=$	5.03	3.10	3.70	9.16	16.53	1.85	4.03	4.51	6.97	17.89	11.08	16.87	1.90	7.18	10.43	6.92	17.89	4.10
NH_4^+	0.58	0.54	0.65	1.54	4.31	0.31	0.86	0.75	1.13	1.72	1.79	1.88	0.20	0.72	1.54	0.98	4.31	0.77
ng/m³																		
Li	0.92	0.31	0.69	0.97	0.92	0.40	0.55	1.15	1.13	0.70	0.76	0.72	0.15	0.83	0.30	0.57	1.15	0.25
Be	0.06	0.04	0.03	0.04	0.03	0.04	0.04	0.06	0.07	0.04	0.04	0.04	0.02	0.06	0.03	0.04	0.07	0.01
Sc	0.84	n.a.	0.82	0.03	0.38	2.69	0.24	2.61	4.12	0.10	1.00	0.73	0.42	1.02	1.79	1.10	4.12	0.86
Ti	58.08	28.16	55.06	60.66	43.66	50.45	43.59	87.21	77.30	41.64	49.82	44.50	17.98	91.01	17.87	45.10	91.01	16.15
V	4.72	3.16	3.44	3.71	3.52	2.55	3.44	4.37	5.14	8.57	4.65	5.19	1.34	3.65	2.83	3.59	8.57	1.34
Cr	2.82	1.84	4.02	4.80	4.90	< d.l.	1.49	2.71	3.06	5.63	2.28	1.93	0.42	1.90	1.11	2.15	5.63	1.46
Mn	29.19	14.38	30.58	35.45	32.31	19.23	20.97	30.85	36.86	27.50	25.90	23.57	8.13	29.51	12.85	21.61	36.86	7.91
Co	0.36	0.20	0.34	0.38	0.31	0.25	0.23	0.42	0.42	0.28	0.27	0.25	0.08	0.35	0.11	0.24	0.42	0.08
Ni	2.68	2.05	4.33	4.58	4.46	3.12	1.85	2.19	2.78	4.39	2.99	3.12	1.18	1.63	1.47	2.81	4.90	1.20
Cu	5.68	4.60	7.64	8.93	9.89	4.24	3.42	5.68	9.84	10.69	7.29	6.46	3.26	6.71	5.82	5.98	11.12	2.28
Zn	67.15	73.18	88.72	120.21	143.00	34.60	30.03	58.59	112.05	130.90	97.85	87.91	23.14	56.53	70.14	71.53	151.49	36.14
Ga	0.63	0.31	0.52	0.84	1.24	0.29	0.40	0.63	0.75	0.68	0.67	0.84	0.09	0.54	0.38	0.47	1.24	0.23
As	3.41	2.02	2.76	5.89	5.33	1.75	1.10	2.82	3.21	5.31	5.06	4.48	0.52	2.18	1.95	2.81	5.69	1.52
Se	0.77	0.36	0.80	1.53	0.96	0.53	0.69	0.98	1.61	0.59	0.76	0.53	0.35	0.85	0.18	0.76	1.69	0.37
Rb	2.48	0.97	1.76	2.47	2.54	0.91	1.34	3.09	3.24	2.56	2.52	2.29	0.38	2.24	1.44	1.72	3.24	0.79
Sr	6.15	2.25	4.02	4.79	3.33	2.41	3.67	7.40	6.26	3.68	3.71	3.71	1.05	5.31	1.44	3.27	7.40	1.41
Cd	0.66	0.31	0.39	0.77	1.11	0.26	0.33	0.44	0.65	1.13	0.89	0.88	0.15	0.31	0.40	0.47	1.13	0.28
Sn	1.28	0.84	1.58	2.40	3.02	0.81	0.96	1.42	2.32	3.88	2.50	2.44	0.51	1.56	1.29	1.55	3.88	0.77
Sb	1.13	0.95	1.84	2.42	2.81	0.62	0.92	1.51	2.69	3.01	2.45	2.02	0.87	1.69	1.53	1.68	6.86	1.13
Cs	0.34	0.14	0.24	0.38	0.43	0.17	0.16	0.42	0.48	0.41	0.33	0.31	0.04	0.23	0.25	0.25	0.48	0.13
Ba	13.95	8.97	12.89	19.39	11.15	5.04	8.83	17.62	19.88	10.29	9.92	9.09	4.20	15.31	7.79	10.22	23.48	4.41
La	0.77	0.33	0.63	0.68	0.37	0.24	0.49	0.93	0.94	0.48	0.58	0.58	0.15	0.70	0.25	0.45	0.94	0.20
Ce	1.47	0.62	1.11	1.31	0.69	0.63	0.96	1.87	1.88	0.90	0.97	0.94	0.40	1.39	0.55	0.87	1.88	0.38
Pr	0.17	0.07	0.11	0.14	0.06	0.06	0.11	0.22	0.19	0.07	0.08	0.08	0.01	0.15	0.03	0.08	0.22	0.05
Nd	0.56	0.24	0.33	0.43	0.17	0.15	0.37	0.71	0.64	0.27	0.32	0.30	0.08	0.55	0.12	0.28	0.71	0.16
Sm	0.13	0.06	0.03	0.05	0.01	< d.l.	0.08	0.15	0.13	0.06	0.07	0.06	0.02	0.13	0.03	0.06	0.15	0.04
Eu	0.04	0.03	0.01	0.01	< d.l.	0.01	0.04	0.04	0.04	0.02	0.02	0.02	< d.l.	0.02	< d.l.	0.02	0.04	0.01
Gd	0.13	0.07	0.01	0.04	< d.l.	< d.l.	0.09	0.15	0.14	0.06	0.07	0.07	0.02	0.13	0.02	0.07	0.15	0.04
Tb	0.02	0.01	< d.l.	< d.l.	< d.l.	< d.l.	0.01	0.02	0.02	< d.l.	< d.l.	< d.l.	< d.l.	0.02	< d.l.	0.01	0.02	0.01
Dy	0.11	0.08	< d.l.	< d.l.	< d.l.	< d.l.	0.08	0.13	0.12	0.02	0.03	0.02	< d.l.	0.12	0.02	0.06	0.13	0.04
Ho	0.02	0.01	< d.l.	< d.l.	< d.l.	< d.l.	0.01	0.02	0.02	< d.l.	0.01	< d.l.	< d.l.	0.02	< d.l.	0.01	0.02	0.01
Er	0.05	0.03	< d.l.	< d.l.	< d.l.	< d.l.	0.04	0.06	0.06	0.01	0.01	0.01	< d.l.	0.06	0.01	0.02	0.06	0.02
Tm	0.02	0.02	< d.l.	< d.l.	< d.l.	< d.l.	0.02	0.02	0.02	< d.l.	< d.l.	< d.l.	< d.l.	0.01	< d.l.	0.01	0.02	0.01
Yb	0.05	0.03	< d.l.	< d.l.	< d.l.	< d.l.	0.03	0.06	0.06	0.01	0.01	0.01	< d.l.	0.05	0.01	0.02	0.06	0.02
Lu	0.02	< d.l.	< d.l.	< d.l.	< d.l.	< d.l.	< d.l.	0.02	0.02	< d.l.	< d.l.	< d.l.	< d.l.	0.02	< d.l.	0.02	0.02	0.00
Hf	0.49	0.63	0.47	0.57	0.48	0.42	0.56	0.51	0.56	0.34	0.37	0.35	0.32	0.64	0.58	0.48	0.64	0.09
Ta	< d.l.	0.05	0.02	0.04	< d.l.	< d.l.	< d.l.	0.03	0.09	< d.l.	< d.l.	< d.l.	< d.l.	0.04	< d.l.	0.04	0.10	0.03
W	0.66	0.86	1.08	0.83	1.30	0.60	0.40	0.79	0.95	1.35	1.68	0.96	0.56	1.04	0.44	0.79	2.06	0.40
Tl	0.14	0.07	0.13	0.28	0.39	0.12	0.08	0.18	0.37	0.33	0.34	0.34	0.02	0.13	0.18	0.17	0.39	0.11
Pb	27.65	14.45	24.37	45.34	62.50	6.84	13.76	28.87	44.71	57.39	44.36	40.47	4.44	14.46	28.96	24.63	62.50	16.26
Bi	0.51	0.25	0.64	0.96	1.38	0.24	0.73	0.55	0.95	1.65	0.99	0.97	0.19	0.41	0.74	0.57	1.65	0.36
Th	0.17	0.09	< d.l.	0.09	< d.l.	0.05	0.04	0.23	0.22	< d.l.	< d.l.	< d.l.	< d.l.	0.29	0.08	0.13	0.29	0.07
U	0.17	0.15	< d.l.	< d.l.	< d.l.	< d.l.	0.15	0.21	0.18	0.04	0.04	0.05	< d.l.	0.19	0.06	0.10	0.21	0.06
µg/m³																		
Mineral	13.76	5.11	10.25	11.55	7.67	8.49	8.20	16.46	14.57	7.77	9.36	8.72	3.11	15.70	3.15	8.25	16.46	3.16
OM+EC	7.03	6.93	11.23	11.03	11.78	4.53	4.26	8.72	10.42	9.01	18.16	13.40	5.13	11.67	9.05	8.96	18.16	3.14
SIC	10.08	7.56	10.36	18.88	36.99	3.99	6.23	9.53	12.73	25.86	17.42	22.41	4.18	10.88	17.03	12.54	36.99	7.03
Marine	1.40	0.56	0.79	0.72	1.04	1.62	2.07	0.70	0.56	1.31	1.74	1.66	1.08	0.81	0.62	1.06	2.33	0.43
Trace metals	0.24	0.18	0.25	0.33	0.34	0.15	0.15	0.28	0.35	0.33	0.27	0.25	0.07	0.27	0.18	0.21	0.37	0.08

Too small to read

Table 1